

# Hybrid SPV/ Wind Mini-Turbine UPS

S. Jayasimha and T.P. Kumar

Signion Systems Ltd.

71&72, Anrich Industrial Estate, IDA Bollaram

Medak District, A.P., India 50232. e-mail:[info@signion.com](mailto:info@signion.com)

## Abstract

An adaptation of an SPV-UPS relay controller, reported earlier, allows a small variable-speed wind turbine's power to minimize grid usage and daytime monsoon outages, while increasing, at sufficient wind speed, nighttime back-up.

## 1. INTRODUCTION

Wind mini-turbines are typically three-phase permanent-magnet machines, whose no-load output voltages and frequencies vary linearly with wind-speed. This varying output can directly be used in very limited applications (such as heating), but, in general, cannot be used with low-cost mass-produced appliances. An example is a 4-pole Virya 3.3 turbo-generator (Figure 1), described by its designer (Kragten [1]) as:  $U = \frac{9.5 \lambda w}{\pi D}$  Volts,  $f = \frac{2 \lambda w}{\pi D}$  Hz,  $n = \frac{\lambda w}{\pi D}$  rps, where  $U$  is the phase voltage supplied at a frequency  $f$ ,  $n$  is the rotor's speed,  $w$  is the wind velocity's normal component in m/s,  $D$  the swept diameter ( $D=3.3$ m) and  $\lambda$  the design tip speed ratio ( $\lambda=5$ ). At  $w=3$ m/s, the no-load phase rms voltage, with frequency 2.9Hz, is 13.75V. When  $w=40$ m/s, the no-load phase voltage, with frequency 38.7Hz, is 183V (because a boom-tail hinged lifting vane deflects the rotor away from the high ( $>>40$ m/s) magnitude wind vector).



Figure 1. Installed Virya 3.3 turbine (height=20m)

Location Latitude, Longitude	Year	Altitude (mASL)	Sensor height (m)	Annual mean $w$ (m/s)	Monsoon mean $w$ (m/s)	Monthly standard deviation (m/s)	Monsoon standard deviation (m/s)
Naseerabad [2] 17°11'N, 77°55'E	1995-96	664	25	5.84	6.6	0.74	0.72
			20	5.67 <sup>#</sup>	6.41 <sup>#</sup>		
Hakimpet Airport† 17°53'N, 78°51'E	1958-67	613	~10	4.19	6.53	0.54	0.72
			20	4.58 <sup>#</sup>	7.15 <sup>#</sup>		
Hyderabad Airport† 17°27'N, 78°28'E	1958-70	545	7.4	3.33	5.2	1	0.80
			20	3.79 <sup>#</sup>	5.92 <sup>#</sup>		
Signion* 17°52'N, 78°22'E	1995-96	600	20	4.68	6.5	1	0.71

† Indian Meteorological Department (IMD) records

# Normalized to 20m sensor height ( $h_2$ ), using power law index  $\alpha=0.13$ , in  $w_2/w_1=(h_2/h_1)^\alpha$  from measured speeds ( $w_1$ ) at actual heights ( $h_1$ )

\* Computed by averaging #

Table 1. Annual and monsoon wind speeds

An approximate mean of  $w$  at the chosen open-terrain location is obtained by averaging nearby wind monitoring stations records (Table 1). Accounting for 12m and 7.5m mast and structure (Figure 1) heights, the mean  $w$  at the generator may be 4.7m/s with standard deviation under 1m/s, at which wind power is 1056W, i.e.,  $P=\rho A w_r^3$ ,  $A$ =swept area,  $w_r$ =rms wind speed and  $\rho$ , the mean regional air density, is 1.092kg/m<sup>3</sup>.

With conversion efficiency 0.2, mean electric power and energy delivered are about 211W and 1851kWh/annum. During the 1995-96 monsoon (June 1-August 31), a 6.5m/s [2] mean  $w$  yielded mechanical power of 2594W, providing electric power and energy of 519W and 1145kWh (nearly 2/3 the annual yield) respectively. Figure 2 also shows that winter night winds may provide significant energy (when rectified star-connected wind-generator windings' open-circuit voltage exceeds the UPS's minimum battery voltage).

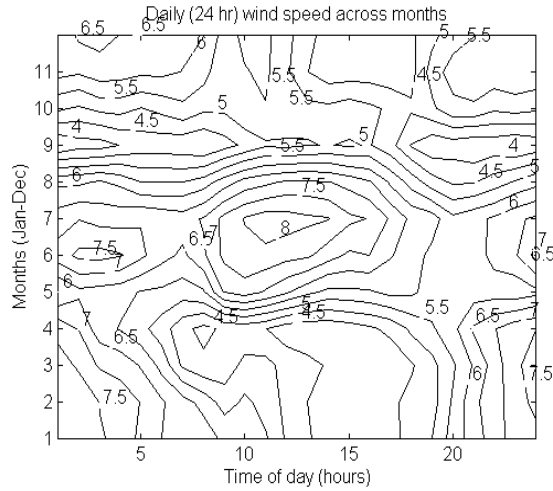


Figure 2. Hourly mean velocity (m/s) contours (from [2]) at Naseerabad, 25m sensor height

## 2. SPV-UPS CONTROLLER

A previously reported relay-controller [3] minimizes daytime grid energy and actuation costs by measuring the SPV's open-circuit voltage,  $V_s^{oc}$ , and adjusting the battery state-of-charge (SOC) and voltage to the SPV array's peak power voltage,  $V_s^{mp}$ , using either grid or SPV energy. In the pertinent example, a 42-module solar photovoltaic (SPV) array ( $M=6$  parallel strings, each with  $N=7$  serial modules), each module comprising 36 serial cells, with array  $V-I$  and  $P-I$  characteristics, at 20-100% STC solar intensity ( $1\text{kW/m}^2$ ), shown by Figure 3, is connected to the dc-bus of a 5kW uninterruptible power supply (UPS) as shown in Figure 4.

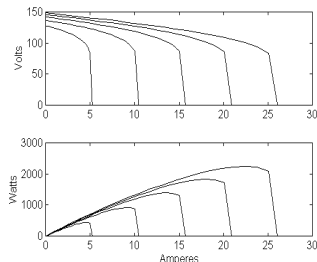


Figure 3. SPV array's voltage and power vs. current at 20% multiples of STC solar intensity

## 3. WIND MINI-TURBINE INCLUSION

An SPV array and a small wind generator<sup>1</sup> may both<sup>2</sup> be coupled to an off-the-shelf UPS (using relays and a relay controller) via Figure 5's circuit, whose chief benefit is the transfer

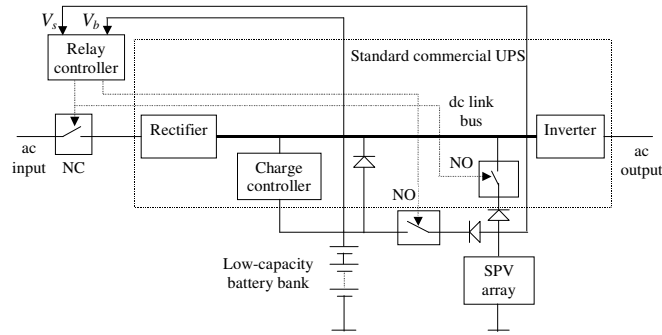


Figure 4. Line diagram of photovoltaic UPS

<sup>1</sup> A wind generator's speed-dependent inertial energy, ranging between 980-13210J for a rotating Virya 3.3, increases stored energy (as do electrochemical capacitors in [4]) by a factor of 10-100 beyond the UPS dc bus's capacitive energy (100J for  $C=0.02\text{F}$ ,  $V_{dc}=100\text{V}$ ), reducing the frequency of peak-current (e.g., inrush and locked-rotor currents associated with induction motor start-up) induced outages.

<sup>2</sup> Suppose investments  $I_s$  and  $I_w$  in SPV and wind infrastructure respectively generate annual (or monsoon) mean daytime powers  $P_s$  and  $P_w$ , with variances  $\sigma_s^2$  and  $\sigma_w^2$ . Minimizing an overall variance-to-mean-square ratio (for uncorrelated SPV and wind power),  $[(\alpha_s \beta_s)^2 r^2 + (\alpha_w \beta_w)^2 (1-r)^2] / [\alpha_s r + \alpha_w (1-r)]^2$ , with respect to  $r$  ( $r/[1-r]=I_s/I_w$ ,  $\alpha_s=P_s/I_s$ ,  $\alpha_w=P_w/I_w$ ,  $\beta_s=\sigma_s/P_s$  and  $\beta_w=\sigma_w/P_w$ ) leads to a reliable solution [5] for  $r$  (a root of  $a \cdot r^2 + b \cdot r + c$ , with  $a=(\alpha_w - \alpha_s) \cdot (\alpha_s \beta_s^2 + \alpha_w \beta_w^2)$ ,  $b=\alpha_w \cdot [\alpha_s \cdot (\beta_w^2 - \beta_s^2) - 2 \cdot \alpha_w \beta_w^2]$ ,  $c=\alpha_w^2 \cdot \beta_w^2$ ). From local wind and solar data [2,6] (assuming

of wind power to the load even when the star-connected 3- $\phi$  generator's rectified voltage is very low. At night, SPV modules' bypass diodes carry the wind-supplied load current component (thereby preventing SPV cell damage [8]). The relay controller's features include:

- Daytime battery charging (to  $V_s^{mp}$ , based on measured  $V_s^{oc}$ ) from the series-connected SPV/rectified wind generator, with open circuit voltage<sup>3</sup>  $V_{s+w}^{oc}$ . For  $w < 3\text{m/s}$ , the hybrid and SPV-only systems behave identically.
- Wind-augmented ( $w > w_{cut-in}$ ) grid-interactive nighttime power delivery (and back-up)
- Automatic over-voltage protection hardware (solid-state relay with manual reset)

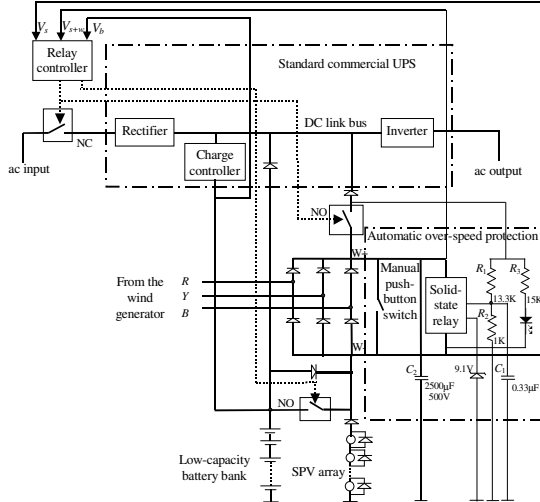


Figure 5. Line diagram of hybrid Wind-SPV UPS

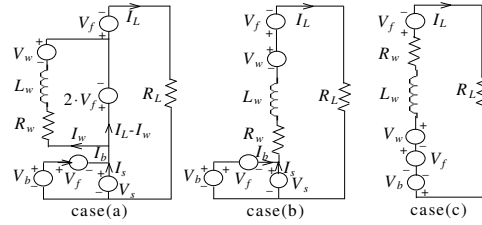


Figure 6. Hybrid SPV-wind equivalent circuits

Daytime equivalent circuits are shown as cases (a), (b) and (c) in Figure 6: (a) occurs at speeds below  $w_{cut-in}$ <sup>4</sup>, where all the 3- $\phi$  rectifier bridge's diodes are forward biased ( $V_w \leq I_w \cdot R_w - 2 \cdot V_f$ ) and the wind generator's load power contribution is zero, while (b) occurs when the rectifier bridge operates normally (i.e.,  $V_w > I_w \cdot R_w$ ), with positive wind generator power. With load power,  $P_L = 2.25\text{kW}$ ,  $w_{cut-in}$  ( $= 4.5\text{m/s}$  i.e.,  $0.0891 \cdot R_w \cdot P_L / V_{dc}$  for a Virya 3.3, with  $R_w = 2.5\Omega$  and  $V_{dc} = 112\text{V}$ ) can be made small by selecting a UPS with a sufficiently high dc-link voltage, i.e., given  $P_L$ , reduce the parallel ( $M$ ) strings and increase each string's series ( $N$ ) SPV modules. In cloudy and windy conditions, when  $(I_L - I_b) > I_{sc}$ ,  $I_L - I_b - I_{sc}$  is bypassed by SPV modules' diodes (case c,  $I_{sc}$  being the array's short-circuit current). When the sum of SPV and rectified wind voltages, under load, exceeds the dc bus's voltage limit, a solid-state relay<sup>5</sup> (SSR at Figure 5's lower right) shorts the generator's windings. This allows the mechanical safety system's activation force to be increased (eg., by weighting the hinged vane that turns the rotor away from large wind vectors), thereby minimizing mechanical power wasted.

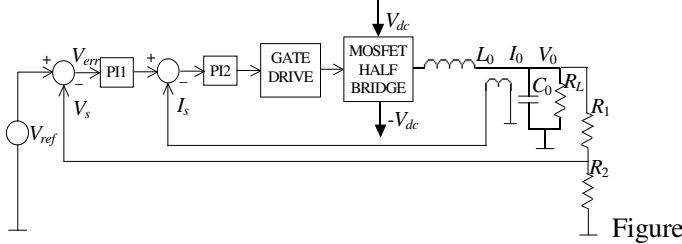
efficiencies  $\eta_s = 0.1$ ,  $\eta_w = 0.2$ ,  $r_{annual} = 0.82$  and  $r_{monsoon} = 0.66$ . For negatively correlated wind and SPV variations,  $r$  is about 0.66. The installation depicted in Figure 1, where  $P_w$  is lower than in [2], has  $r = 0.9$ . Because reduced summertime SPV power (due to temperature rise [7] and clouds) is supplanted by wind power, the hybrid system's fixed SPV array's usual latitude tilt (pg. 28 in [8]) may be skewed southward to enhance wintertime power.

<sup>3</sup> A second-order filter, with  $|H(\omega)| = 1 / (1 + (\omega/\omega_c)^{2N})^{1/2}$ ,  $N=2$ ,  $\omega_c = 6\pi$ , provides attenuations of 30dB at 18Hz and 54dB at 66Hz and suppresses the peak-to-peak ripple of  $[3 \cdot (1 - \sqrt{3}/2) / \pi] \cdot V_w^{dc}$  in  $V_{s+w}^{oc}$ .

<sup>4</sup> At speeds beyond the starting speed, each winding's alternating current is non-zero for phase angles (in radians) in  $(\delta + \pi/3, \delta + 2\pi/3)$  or  $(\delta + 4\pi/3, \delta + 5\pi/3)$ , where  $\delta \approx 4 \cdot \lambda \cdot w \cdot L / (R \cdot D)$ . Since the winding's reactance in the fundamental frequency range of 2.9-10.6Hz is small compared to  $R$  when  $w < 11\text{m/s}$ ,  $w_{cut-in}$  is computed based only on  $R$ .

<sup>5</sup> e.g., in Figure 5's SSR, with turn-on voltage between 1-3V, and input resistance of  $1\text{k}\Omega$ , actuates, when the 1:26.6 ratio potentiometer sense point exceeds 10.1-12.1V (i.e., with a  $V_{s+w}^{oc}$  range of 269.26-322.46V). Daytime and nighttime no-load actuation speeds are 13.12-17.86m/s (for  $V_{s+w}^{oc} = 122\text{V}$ ) and 23.99-28.73m/s respectively.

#### 4. HYBRID UPS CONTROLLER REALIZATION



7. Inverter controller

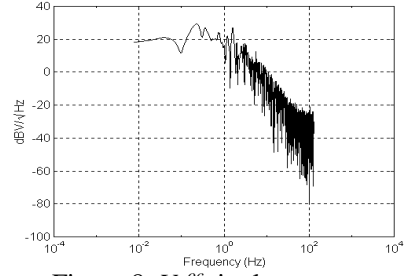


Figure 8.  $V_w^{oc}$  ripple spectrum

Voltage and current feedback inverters' (Figure 7) wide-band response<sup>6</sup> provides good line regulation [11] even when the UPS's dc bus capacitance<sup>7</sup> doesn't suppress  $V_w$ 's high-frequency components (Figure 8). The controller minimizes grid energy and actuation (battery and relay life) costs as follows:

- Momentary disconnects the series combination of the SPV array and star-rectified wind generator from the UPS's dc link bus and the battery to allow  $V_s^{oc}$  and  $V_{s+w}^{oc}$  to be measured (ac mains, or, if absent, the battery-bank, supporting the load).
- Wind-augmented SPV power flows to the battery bank and/ or load<sup>8</sup> during daytime.
- The battery's SOC is adjusted so that operation at  $\max(V_s^{mp}+2\cdot V_f, V_b^{min})$  occurs.  $V_b^{min}$  is the minimum battery operating voltage of the UPS (below which an audible alarm sounds). A proportional charge controller computes  $\rho=0.9\cdot\rho+K\cdot[V_{target}+2\cdot V_f-V_b]$ ,  $0<\rho<1$ , where  $V_{target}$  is the battery's full charge voltage,  $V_b^{full-charge}$ , when  $V_{s+w}^{oc} < V_s^{min}$  and to  $L(V_s^{oc})$  otherwise, where  $L(\cdot)$  linearly maps  $V_s^{oc}$  to  $V_s^{mp}$  ( $V_s^{oc}$  is measured at a PWM period's beginning).
- $K$ , a function of the UPS's battery charging current,  $I_c$ , and its capacity (in AH), is based on the controller tracking  $V^{mp}$  and yet utilizing some SPV energy as the sun ascends. The maximum mean ac mains duty cycle,  $\rho_{av}$ , for the ascending sun period,  $T_r$ , is  $(S_{as}-S_{sr})/(I_c\cdot T_r)$ , where  $S_{as}$  is the desired battery SOC (in AH) at STC intensity,  $S_{sr}$ , the SOC at sunrise and  $I_c$ , the battery charging current. To minimize UPS tripping likelihood as the sun ascends,  $K=[1-\kappa(V_b-V_b^{min})]$ , where  $\kappa$  is a gain scheduling multiplier. For example, at  $V_b^{min}$ ,  $\rho=1$ . Grid power (through the UPS's rectifier and charge controller) charges the battery with duty cycle  $\rho$  to the desired SOC. The normally open (NO) relay of Figure 9 is activated after sampling  $V_{s+w}^{oc}$  (this relay is deactivated, whenever  $V_{s+w} > V_b^{max}+V_f$ , to avoid excessive charging current or when  $\rho=1$ , at the current PWM period's end, in order to sample  $V_{s+w}^{oc}$  again), thereby allowing SPV and wind energy to augment ( $C_2$  in Figure 5 charges during the AC ON cycle and discharges to the load during the OFF cycle) battery SOC build-up.
- A PWM period of 20s extends relay life and ensures a negligible steady state performance loss (due to  $V_{s+w}^{oc}$  measurement). To avoid tripping the UPS when SPV and wind power are inadequate and ac mains absent, the PWM period,  $\tau$ , is reduced to 5s when consecutive sample  $V_{s+w}^{oc}$  are different, e.g., due to clouds or wind gusts; also, at a PWM period's expiry

<sup>6</sup> To provide sufficient harmonic suppression [9] and to compensate for short [10] voltage sags and swells, the closed-loop response of 50Hz sine wave inverters, using Figure 7's voltage and current PI control, exceeds 150Hz.

<sup>7</sup> For example, a 100V, 19800 $\mu$ F dc bus, with typical 3 $\Omega$  load, has a roll-off of 20dB/decade beyond 1.5Hz.

<sup>8</sup> The battery charger voltage being set below  $V_{mp}^{min}$  (95% of  $V_{mp}^{STC}$ ), the batteries float at  $V_{mp}$  ensures maximum SPV power utilization. For an example 3kW array ( $V_{mp}=100$ V, noontime  $I_{mp}=30$ A) in series with a 1kW wind generator, with assumed battery charging and discharging efficiencies,  $\eta_{ch}$  and  $\eta_{dch}$ , of 0.9; for  $I_L=45$ A (5kW UPS with a dc bus voltage of 112V), duty cycle  $\rho=(I_L I_{mp})/[(\eta_{ch}\cdot\eta_{dch}\cdot I_{mp})+I_L\cdot I_{mp}]$  is 0.38 implying that 872W of SPV power is delivered via battery and 1776W is streamed directly to the load, with a net efficiency of 88%, while wind contributes 617W, and ac mains, 2291W. Nighttime ac mains power consumed is about 4671.5W, while wind generator and batteries deliver 288W and 596W respectively to the load, at a mean wind speed of 4.5m/s.

and postponing, when  $V_s < V_s^{min}$ ,  $V_b < V_b^{min}$  and  $V_{s+w} > V_b^{min}$ , hybrid source-to-dc bus disconnection delays SPV-adaptive battery charging and minimizes outages.

- A sluggish  $V_b$  response to an active ac mains relay (excess hybrid power limiting battery charging rate) indicates loss of grid power and demand side management (DSM) is initiated.

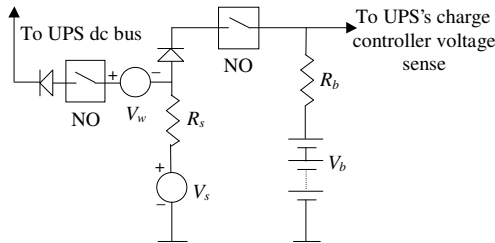


Figure 9. Hybrid source battery charging

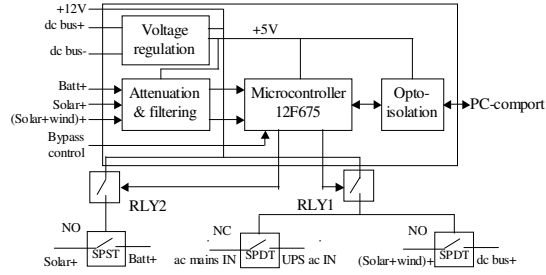


Figure 10. Relay controller schematic

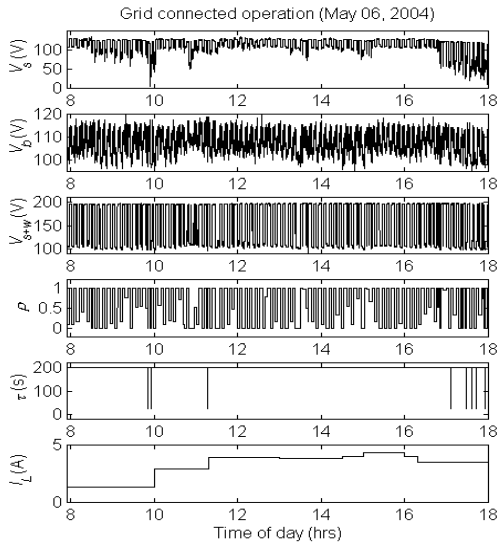


Figure 11. Grid-connected operation

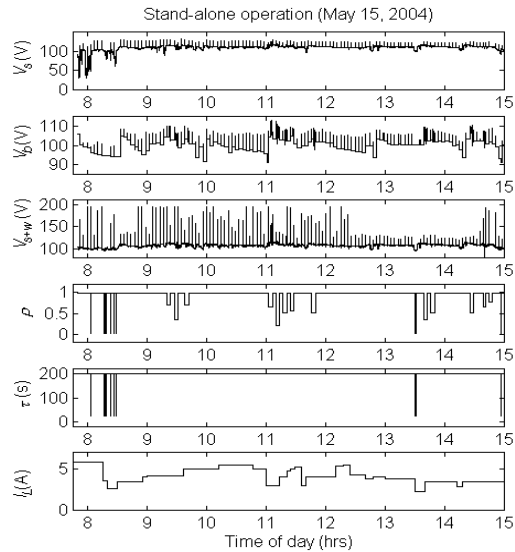


Figure 12. Stand-alone operation until trip

Figure 10 shows a realization of a three-relay controller using a low-cost microprocessor. Figures 8 and 10 of [3] show diurnal data for grid-connected and stand-alone SPV only operation, for a load current,  $I_L$ ,  $\sim 5A$  at 230Vac. Figure 11, showing daytime data for grid-connected operation of the hybrid UPS, illustrates the benefit of the wind turbine on an overcast, stormy day, when 2.7kWH (of 7.8kWH demand) was supplied by the hybrid system, while the ac mains supplied 5.8kWH to cover the deficit (including battery charging and UPS inefficiency). Figure 12 shows the hybrid system's demand-side managed stand-alone operation on a day that began with scattered clouds and strong winds, giving way to sunny skies, followed by an overcast afternoon. 5.5kWH was supplied till the system tripped. Starting an induction motor (load current evolution shown in Figure 13's lower traces) causes the dc bus capacitor to discharge and recharge exponentially in the SPV-only system as in (a). With the same insolation, (b) shows an sag (due to the mini-turbine's winding inductance) of smaller magnitude (6.75J kinetic energy transfer accounting for the 3.2V difference), demonstrating the hybrid system's greater tolerance to load-induced transients.

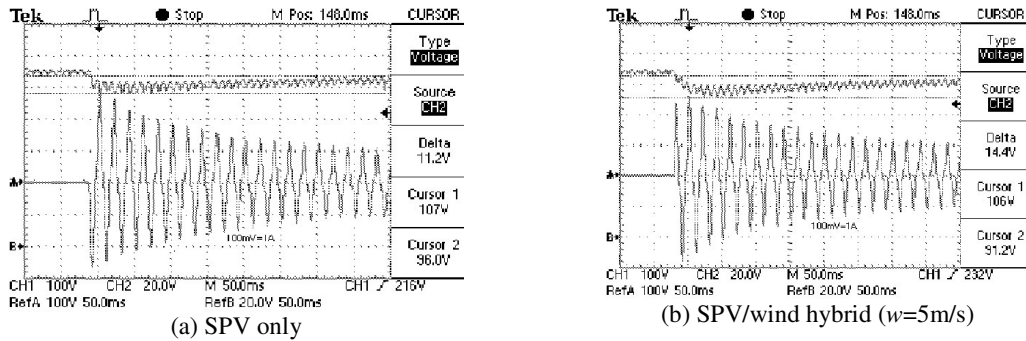


Figure 13. Peak-load induced dc bus voltage sag (stand-alone mode)

## 5. CONCLUSION

Wind mini-turbines, driven by cost-savings, power quality, reliability and security considerations, will be popular by this decade's end. Their early acceptance in India may be facilitated by the simple method described. A wind mini-turbine may be an ideal complement to an SPV array in certain geographical regions with unreliable, under-supplied or under-rated [12] electrical grids; in some cases, the cost savings associated with reduced storage (e.g., battery) capacity may well pay for the additional system component.

*Acknowledgment:* We thank V.V. Krishna (research) and S. Krishnamurthy (data analysis).

## REFERENCES

- [1] Ruurd van der Meulen, "De Formule Virya," [http://www.wot.utwente.nl/documents/articles/2003\\_virya-formule.pdf](http://www.wot.utwente.nl/documents/articles/2003_virya-formule.pdf), March 2003.
- [2] S. Rangarajan, *Wind Energy Resource Survey in India*, Vol.5, Allied Publishers, Mumbai, 1998, pp. 327-335.
- [3] S. Jayasimha and T.P. Kumar, "Photovoltaic UPS," *Proc. of IEEE Tencon 2003 (Convergent Technologies for Asia-Pacific Region)*, pp. 1419-1423, Allied Publishers, Mumbai, ISBN 0-7803-8162-9.
- [4] S. Ranade, N. Clark, S. Atcitty, J. Boyes, "Extending DER Transient Loadability Using Electrochemical Capacitors," <http://www.sandia.gov/ess/Publications/Conferences/2001/SatishRanade.pdf>.
- [5] M.D. Ilic, F.D. Galiana and L.H. Fink (Eds.), *Power Systems Restructuring: Engineering and Economics*, Kluwer Academic Publishers, May 1998, ISBN: 0792381637, pp. 75-78.
- [6] A. Mani and S. Rangarajan, *Solar Radiation Over India*, Allied Publishers, Mumbai, 1982, pp. 35-46, 129-140.
- [7] D.L. King, J.A. Kratochvil, and W.E. Boyson, "Temperature coefficients for PV modules and arrays," *Proc. of 26<sup>th</sup> IEEE PV Specialists Conference*, Sept., 1997
- [8] *Stand-alone Photovoltaic Systems - A handbook of recommended design practices*, SAND87-7023, NTIS, U.S. Department of Commerce, VA, 1990, pp. 25-27.
- [9] N. Mohan, T.M. Undeland, W.P. Robbins, *Power Electronics: Converters, Applications and Design*, Wiley, 1989, pp. 268-270.
- [10] IEEE Standards: 519-1992, 2002, *IEEE Standard Practices and Requirements for Harmonic Control in Electrical Power Systems*, ISBN 1-5593-7239-7 and 1159-1995, 2001, *IEEE Recommended Practice for Monitoring Electric Power Quality*, ISBN 1-5593-7549-3.
- [11] S. Buso, S. Fasolo and P. Mattavelli, "Uninterruptible Power Supply Multiloop Control Employing Digital Predictive Voltage and Current Regulators," *IEEE Transactions on Industry applications*, Vol.37, No.6, November/December 2001, pp.1846-1854.
- [12] WADE, *World Survey of Decentralized Energy 2004*, <http://www.localpower.org/pdf/WorldSurveyonDE-2004.pdf>, pp. 33-35.